Adv Polym Sci (2008) 212: 187–225
DOI 10.1007/12_2008_147

Published online: 22 May 2008

Polyfluorene Photophysics

Andy Monkman (✉) · Carsten Rothe · Simon King · Fernando Dias

Organic Electroactive Polymer Research Group, Durham University, South road, Durham DH1 3LE, UK
a.p.monkman@durham.ac.uk

Abstract The fundamental optical properties and processes that occur in the polyfluorenes are discussed. Details are given on the production of singlet and triplet excitons, their emissive decay channels via fluorescence and phosphorescence and non emissive decay via quenching, together with exciton lifetime and quantum yields of production. The interaction of excitons in these polymers is then discussed at length describing exciton migration dynamics, exciton–exciton annihilation processes and delayed fluorescence and the trapping of excitons at defect sites. Photogenerated charge state production is described along with intra-chain charge transfer states in fluorene co-polymers. Finally, sections describing the optical properties of the beta-phase of polyfluorene are given along with amplified spontaneous emission which occurs at high beta phase exciton populations.

Keywords ASE · Charge pairs · Exciton dynamics · Fluorescence lifetime · Keto defects · Phosphorescence · Polyfluorene beta-phase

1
Basic Optical Properties

As the archetypical "blue" emitting polymer, polyfluorene has been studied extensively using a wealth of optical techniques to elucidate its photophysical properties. Moreover, as it is a simple homopolymer that can be synthesized to very high purity, it offers a unique platform to help us understand many aspects of the excited state behavior of conjugated polymers in general. Here we address the main properties associated with excited state, i.e. exciton, behavior and the many possible interactions between excitons that can occur, although this is by no means an exhaustive review.

1.1
Absorption

Measuring the steady state optical absorption and emission properties of any luminescent polymer is the most basic but fundamental photophysical measurement we can make. Figure 1 depicts both the absorption and emission spectra for a series of polyfluorene oligomers and poly[9,9-di-*n*-(2-ethylhexyl)fluorene] (PF2/6), along with the fully rigid ladder type MeLPPP.

Upon photo-excitation, any excess vibrational energy of the fluorophores is transferred to their environment on a subpicosecond time scale [1]. Through this process of vibrational cooling, emission originates from the $S_0^n \leftarrow S_1^0$ transition in accordance with Kasha's rule, causing a Stokes shift, i.e. an energy separation between the peak in absorption and peak of emission. After this rapid vibrational relaxation the polymer can undergo further structural relaxation and exciton migration through the energetic disorder [2–4] of the bulk polymer causing an additional ("apparent") Stokes shift. These latter processes also break the mirror symmetry between $S_0^0 \rightarrow S_1^n$ and $S_0^n \leftarrow S_1^0$ spectra (absorption and emission) as absorption is an instantaneous process allowing all possible states to absorb, whereas on the whole only the lowest energy states emit. Thus, absorption spectra of conjugated polymers are commonly structureless and broad, whereas emission spectra can be well-resolved even at room temperature.

From Fig. 1 it can be seen that as the number of repeat units increases both absorption and emission energies red shift but saturate at around 5–7 repeat units, also the Stokes shift decreases for longer oligomers. This is a result of the strong influence of ring rotations on the excited states and the degree to

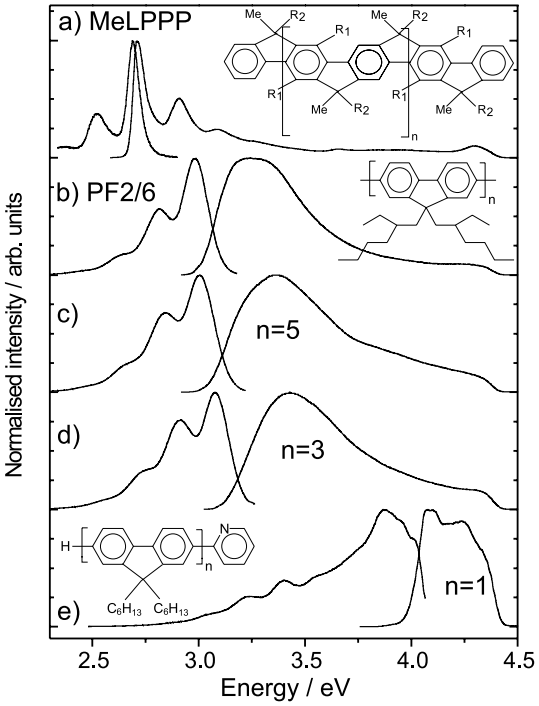

Fig. 1 The steady state absorption and emission spectra of (**a**) methyl ladder type polymer, MeLPPP (**b**) poly[9,9-di-*n*-(2 ethylhexyl)fluorene] (PF2/6, $n \sim 60$) (**c**), pentafluorene (**d**) trifluorene and (**e**) monofluorene measured in dilute toluene solution are compared. The insets depict the chemical structures of each. All spectra were measured in dilute MCH solution

which the rings are free to rotate has a large impact on transition energy, vibronic structure and Stokes shift [4, 5]. This is most clearly exemplified by the fully rigid analogue of PF2/6, ladder type MeLPPP, where no ring rotations can occur. Here the spectra are red shifted with respect to PF2/6 and also both absorption and emission bands are highly structured, but there is virtually zero Stokes shift.

1.2 Emission

Comparing thin film to solution state, we find that there is very little change to the absorption spectrum apart from a small red shift of the whole absorption band, although in solution the band position can be both solvent and time dependent due to conformational changes of the PF backbone in solution [6]. Typical emission spectra of PF2/6 100 nm film at both 295 K and 20 K, excitation at 3.5 eV (10 uJ, 200 ps pulse excitation) are shown in Fig. 2. At low

temperature, the clear vibronic replicas of the electronic transition centered at 2.925 eV are seen. At room temperature this progression is still clearly visible but not as well resolved. A constant energy separation of 175 meV is observed which is associated with a C = C bond stretching mode [7], although high-resolution site-specific fluorescence measurements reveal each replica to be made up of at least three distinct modes [2]. One also sees the characteristic increase of quantum yield at low temperature, rising from ca. 0.3 at 295 K, as measured in an integrating sphere at room temperature [8] to 0.7 at 20 K obtained by comparing areas under the emission spectrum for an estimate of the yield at 20 K. It should be noted also that these values vary greatly between different samples of polyfluorenes and the history of the polymer before measurement. Spectra measured in solution are very similar to that seen in films at low temperature [4].

The lack of mirror symmetry between absorption and emission is indicative of nuclear displacements following excitation [9]. Differences in ground and excited state geometry lead to conformational rearrangement and, for solution samples, to local solvent relaxation following excitation. Both Sluch et al. [10] and Karabunarliev et al. [5, 11] report that the excited state potential of conjugated systems favors ordered planar structures much more strongly than in the ground state. A high degree of torsion [12, 13] between the repeat units and a wide distribution of torsional angles translates directly into a high excited state energy [14] and large energetic spread of excited states (density of states distribution, DOS). Rapid energy relaxation down the DOS gives rise to a red-shift of the emission energy. Consistent with theoretical prediction, the experimentally observed Stokes shifts are pronounced for the highly twisted polyfluorenes and polyphenylenevinylenes (PPV) [13]

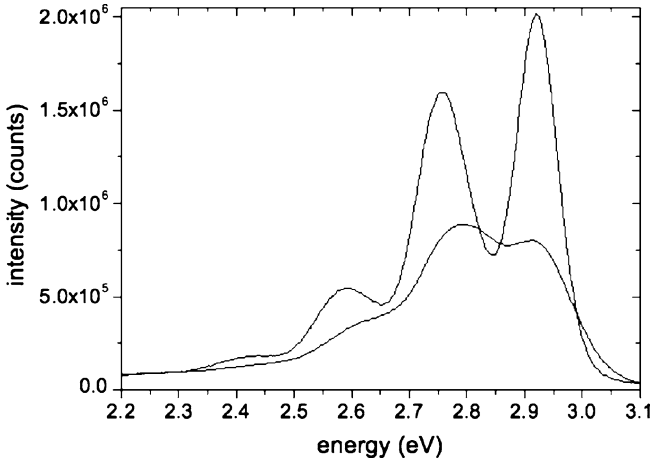

Fig. 2 Room temperature and well resolved 20 K thin film fluorescence spectra of PF2/6

in contrast to the extremely low Stokes shift observed for molecules chemically forced into a planar conformation, i.e. rigid-rod polyparaphenylenes (LPPPs) [15] as seen in Fig. 1. Exciton migration through the DOS will also lead to energetic relaxation and spectral red shifts and will be discussed in Sect. 2.

The planarity of PF2/6 can be controlled by the local environment via its bulky side groups. In Fig. 3 the absorption and emission spectra of dilute PF2/6 in MCH is shown at room temperature and at 77 K (MCH being an excellent glass forming solvent). It is clearly seen that in the low temperature glass, steric distribution and reorganization is hindered and so the absorption band becomes structured and the emission band features sharpen [4].

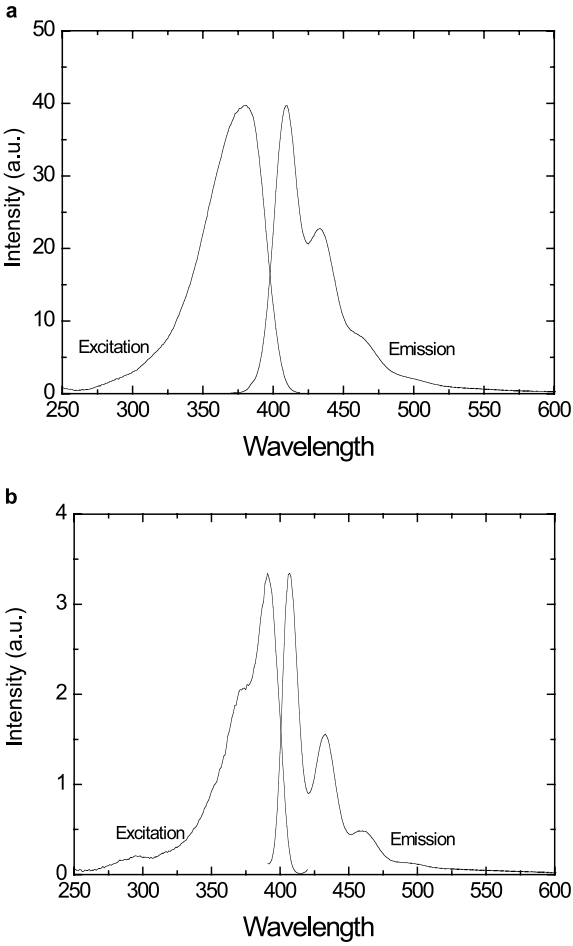

Fig. 3 Excitation and emission spectra of PF2/6 in dilute MCH solution at 295 K (**a**) and 77 K (**b**). Excitation wavelength of the fluorescence measurements was 380 nm

More importantly, the ratio of the intensity of the 0–0 to 0–1 vibrational modes increases. This indicates a decreased Huang–Rhys factor and is ascribed to a low configurational relaxation in the excited state [16]. Thus, torsional motion is hindered by the viscosity of the solvent (glass) and so the excited state has a geometry very similar to that of the ground state. This is also seen in the rigid rod ladder polymer, Fig. 1, where torsional motion is prevented by the inter chain bridging bonds. In this case the line width is narrower but still inhomogeneously broadened, which arises as a result of polydispersity of conjugation lengths and dynamic variation of conjugation lengths [13].

1.3 Fluorescence Lifetime

For most luminescent polymers fluorescence lifetimes lie in the range of 100 ps to 2 ns with multiple decay components, and so the most accurate way to measure this is by the time correlated single photon counting (TCSPC) technique. This is one of the most popular methods to determine excited state lifetimes. The technique makes use of modern pulsed lasers with a very high repetition rate (~80 MHz), typically mode locked Ti:Sapphire lasers. A portion of the excitation pulse is used to generate a START impulse for a time to amplitude converter (TAC) and the remaining light used to excite the sample. The first detected photons emitted by the sample are then sampled by a constant fraction discriminator to generate a pulse that STOPs the TAC. A signal proportional to the elapsed time between START and STOP signals is then produced and the event collected in a memory location with an address proportional to the detection time. After averaging many 1000s of pulses, a histogram of the emission decay is built up which represent the decay curve of the emission. An excellent review on the technique has be written by Becker [17].

Polyfluorenes, like other luminescent polymers show complex fluorescence decays both in thin film and solution, with minor amplitude fast rise and decay components together with a predominant decay time. Although there is still some controversy regarding the origin of the fast components, there is already strong evidence that fast conformational relaxation and energy migration are the cause of this complex behavior. For example, poly(9,9-di-*n*-octylfluorene) (PFO), usually shows a complex decay where sums of two or even three exponential functions are required to achieve excellent fits. This also depends on emission collection wavelength as well.

As a typical example, Fig. 4 shows the decay of PFO in dilute (10^{-5} M) toluene solution with the emission collected at two different wavelengths. A fast component of around 16 ps is found which is more important (greater amplitude) on the onset of the emission band (blue edge), and loses importance when going to longer wavelengths (red edge). Depending on viscosity

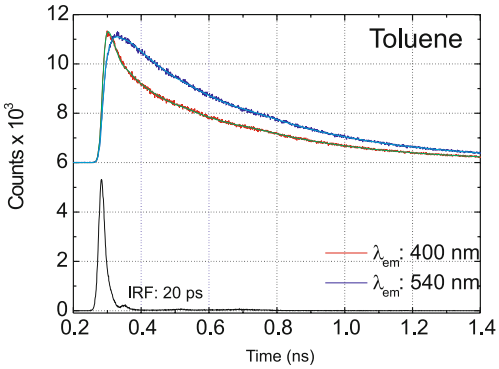

Fig. 4 Time-resolved fluorescence emission decays of PFO in toluene solution obtained at 295 K, with emission collected at 400 nm and 540 nm. Also shown is the instrument response function (IRF) which is deconvoluted with the decay fits to yield a time resolution of 3 ps for the fitted decays

and temperature, this component also appears as a rise time (negative amplitude) when the decay is collected in the emission tail and is the signature of fast conformational relaxations of the polymer backbone. In the rigid ladder polymer, MeLPPP, such fast rise and decay components are not observed, whereas in small fluorene trimers (in dilute solution where processes such as energy migration are not possible) the fast decay and rise components can be readily observed [4, 18, 19]. A minor intermediate component is also observed around 90 ps, which loses importance when going from short to longer emission wavelengths, and is ascribed to weak quenching at impurity sites. A predominant decay time around 360 ps is observed independent of the emission wavelength and attributed to the PFO fluorescence lifetime. Given that the typical PLQY in toluene is 0.8, gives a radiative lifetime of ca. 450 ps. A fast rise of the emission, before decay takes over is clearly observed when the emission is collected at 540 nm. Table 1 summarizes the fitting results, decay times and amplitudes, obtained from time resolved fluorescence decays of PFO in toluene solution and in other organic solvents.

In thin films a similar pattern is observed at short wavelengths, see Fig. 5. The decay is composed of a sum of three exponentials, see Table 2. However, at very long wavelengths, the decay is almost completely dominated by a long component of around 3 ns, attributed to the presence of photooxidized, keto defects or other emissive defects, which are very easily populated by efficient energy migration. This is described in Sect. 1.6. The fast component appears as a rise time of the emission intensity and a component with 349 ps indicates the PFO lifetime.

Table 1 Decay times and amplitudes obtained from time-resolved fluorescence decays of PF2/6 and PFO

Compound	Solvent	λ_{em} (nm)	τ_3 (ps): (A_3)	τ_2 (ps): (A_2)	τ_1 (ps): (A_1)
PF2/6	MCH	400	**40:** (0.11)	–	**371:** (0.89)
		446	**41:** (– 0.29)	–	**373:** (1.00)
PFO	MCH	400	**15:** (0.49)	**71:** (0.07)	**340:** (0.44)
	toluene	400	**16:** (0.54)	**89:** (0.07)	**363:** (0.39)
		540	**16:** (– 0.10)	–	**360:** (1.00)
	chloroform	417			**360:** (1.00)

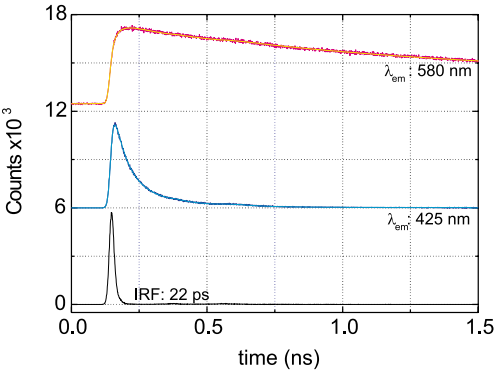

Fig. 5 Time-resolved fluorescence emission decays of PFO films obtained at 295 K, with emission collected at 425 nm and 580 nm. Again IRF also shown

Table 2 Decay times and amplitudes obtained from time-resolved fluorescence decays of PFO in film

		λ_{em} (nm)	τ_3 (ps): (A_3)	τ_2 (ps): (A_2)	τ_1 (ps): (A_1)
PFO	film	425	**36:** (0.57)	**109:** (0.41)	**403:** (0.02)
		580	**28:** (– 0.25)	**349:** (0.28)	**3050:** (0.72)

1.4 Phosphorescence

For all device applications based on organic materials, the energy of the first excited triplet state is of great importance as it is this state that is mainly populated during electrical excitation i.e. via charge recombination [20–22]. An obvious way to measure the triplet energy is by phosphorescence (Ph) detection, i.e. detection of the radiative decay of the first excited triplet state to the singlet ground state. This however, is not easy for most of the polyfluorenes, as the transition is formally spin forbidden. In consequence, the

radiative lifetime of the triplet state is, under most experimental conditions much longer than the non-radiative lifetime thus diffusion activated triplet quenching dominates the decay of the state. To get around this, triplet diffusion has to be restricted, usually by performing the measurements at low temperatures, typically below 20 K. Under continuous excitation, the considerably stronger fluorescence long wavelength tail would completely mask the weak phosphorescence signal. Therefore, pulsed excitation in combination with highly sensitive gated spectroscopy has to be applied, where the collection of the spectrum starts some micro- or milliseconds after the excitation pulse [23–25]. Alternatively, a non-optical excitation method can be used such as pulse radiolysis-energy transfer to measure triplet energies, especially in cases where no phosphorescence can be detected [26, 27].

Figure 6 shows a typical delayed luminescence spectrum of PF2/6 thin film after optical excitation. Delayed fluorescence, which appears at the identical spectral position (2.925 eV) as the prompt fluorescence, see Fig. 2, arises as a result of triplet–triplet annihilation, discussed in Sect. 3.2. The phosphorescence spectrum peaks around 2.2 eV, which sets a lower limit for the triplet energy of polyfluorene. Very similar spectra have been recorded in frozen solutions [24, 28], or using electrical instead of optical excitation pulses [25], and for nearly all other polyfluorene derivatives [23, 29]. Triplet formation in polyfluorenes has been confirmed to be solely via the process of inter system crossing [30] and as the spin orbit coupling of the homopolymer is very low explains why triplet yields are very low in polyfluorenes and most other luminescent polymers [31]. Recently, King et al. succeeded in measuring the triplet yield and intersystem crossing rate for a polyspirofluorene directly in both solution and thin film at low temperature, by developing

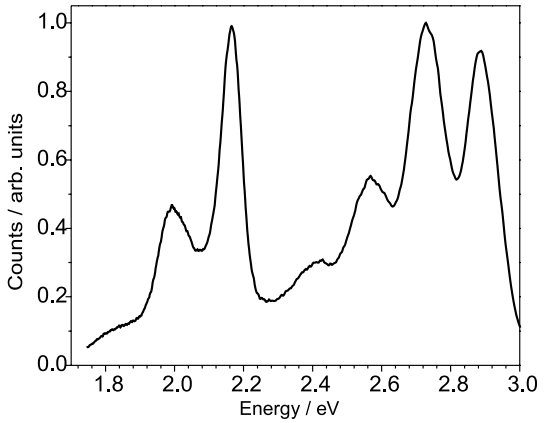

Fig. 6 Delayed luminescence spectrum of a PF2/6 film taken at 20 K with 30 ms delay after excitation and 30 ms detection window. Excitation was provided at 355 nm with 170 ps pulse width using a Nd:YAG laser

a technique based on the femtosecond to nanosecond time resolved measurement of ground state recovery. In solution the triplet yield was found to be 0.05 ± 0.01 with a rate, $k_{ISC} = 5.4 \times 10^7\ s^{-1}$, in films this rises to 0.12 ± 0.02 and is temperature independent. The difference is ascribed to triplet formation from photo generated charge state recombination, see Sect. 3.1. This new methodology gives a powerful way to study triplet creation in films for the first time [32].

As noted above, normally the ISC rates in all luminescent polymers and especially the polyfluorenes are very low giving triplet yields of less than 0.05. However, there is one special case when the ISC of the polymer can reach ca. 1. This is in the presence of a heavy atom containing dopant, typically an Ir based metal–organic complex. In these guest–host systems, even at low doping levels, the spin–orbit interaction between polymer chain and complex, mediated by π wavefunction overlap, is a resonantly enhanced long range spin–orbit coupling, effective over very large distances. Thus, the spin–orbit coupling on the polymer back bone in the region close to a dopant is very high causing fast efficient ISC. This leads to rapid fluorescence quenching of the excited polymer and concomitant high triplet population, with a yield approaching 1 [33].

Because of its spin-forbidden nature, the decay rate of the first excited triplet state is extremely low, and very difficult to quantify accurately. What can be measured is the phosphorescence lifetime. Typical long time decays for a poly(bi-spirofluorene) (PSBF) are shown in Fig. 6.

In order to arrive at meaningful (exponential) decay rates in such experiments, non-linear triplet quenching by diffusion, has to be avoided. For example, the initial accelerated decay in Fig. 7 is caused by bimolecular triplet–triplet annihilation dominating the decay of the triplets. Similarly, a faster decay is observed at higher temperature, where triplet exciton diffusion to quenching sites is faster than monomolecular decay. Nevertheless, by using low temperatures and low excitation doses exponential decay kinetics are observed yielding radiative decay rates as low as $\sim 1\ s^{-1}$, which sets an upper limit for the triplet excited state lifetime [28, 34].

Of course the triplet lifetime could also be determined by probing the transient triplet absorption signal as a function of time [24, 30], see Sect. 1.5.2. In practice however, the very low signal to noise ratio of such experiments requires the use of rather high excitation doses, which can make triplet annihilation the dominant decay mechanism even in dilute solutions.

The polarization of the phosphorescence of polyfluorene is also of interest because it provides a clue to the quantum mechanical wavefunction of the triplet state and its relationship with the singlet ground state. In common with most planar aromatic systems, the phosphorescence is found to be predominantly polarized out of the plane of the phenyl rings [35]. This orientation of the triplet state perpendicular to the singlet is particularly important when considering the energy transfer between singlet and triplet states or

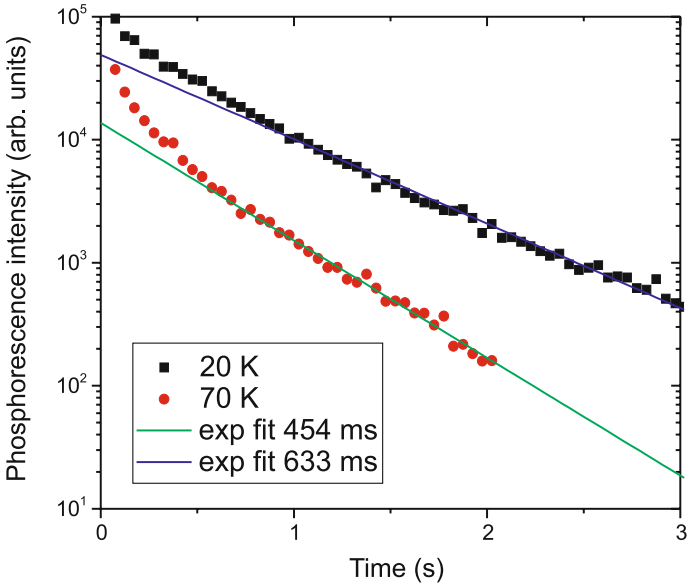

Fig. 7 Phosphorescence intensity as a function of time for a PSBF thin film after pulsed optical excitation and for two temperatures as indicated. The *solid lines* are exponential fits to the late part of the data sets yielding an estimate for the phosphorescence lifetime

the rates of triplet formation by intersystem crossing and the radiative decay rate. The spin forbidden nature of the triplet means that the crossing to the triplet state and its radiative decay are only allowed by mixing of the state with some states of singlet character. The predominantly out of plane nature of the first triplet state compared to the in plane nature of most of the singlet states makes mixing difficult and the rates of triplet formation and radiative decay concomitantly low.

1.5 Transient Absorption

As with the ground state of a molecule, the excited states also have characteristic optical absorption. In a simple system such as the polyfluorene homopolymers, these excited state absorptions can be characterized into three groups, the singlet excited state absorption, the excited state absorption of the first triplet state and the absorption of charged species. The techniques of excited state absorption spectroscopy are particularly useful for investigating non-emissive species such as triplet and charged states and generation from, and interaction with, singlet state. The techniques are also of interest to the device physicist as they are often used to investigate the exciton processes in devices.

1.5.1
Singlet Excited State Absorption S_1–S_n

In common with other conjugated polymers the excited state absorption of the singlet state in polyfluorene homopolymers is a sharp feature peaking just below 1.6 eV shown in Fig. 8. Singlet excited state absorption spectra are typically measured with an ultrafast pump probe system, which can resolve spectra and decays with sub-picosecond resolution [36, 37]. Verification of the feature as the singlet excited state induced absorption has been made by favorable comparison between the decay and excitation dependence of the absorption with the stimulated singlet emission signal and the fluorescence lifetime [38–41]. The excited state absorption of the singlet exciton has been used by many researchers to probe the population of singlet excitons in a number of different types of experiments where it is not possible to use more conventional fluorescence measurements such as at high excitation densities [41, 42], in device structures [39] or most pertinently, where ultrafast time resolution is required [43–45].

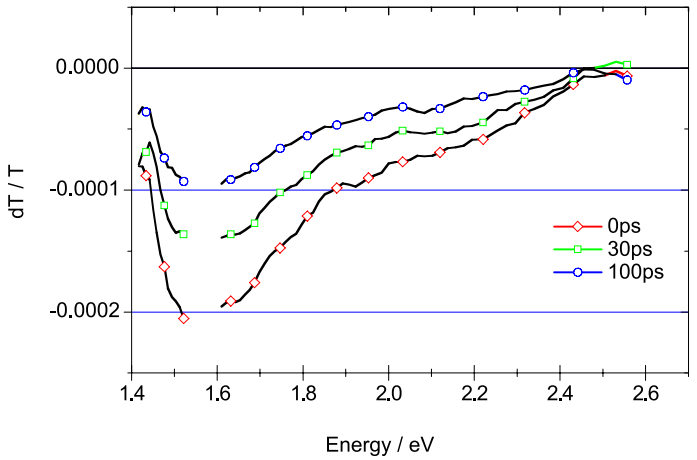

Fig. 8 The excited state absorption of the singlet exciton in PF2/6; the spectra are collected at different delay times after excitation to measure the decay of the state

1.5.2
Triplet Excited State Absorption T_1–T_n

The transient triplet absorption for the common polyfluorene PF2/6 is shown in Fig. 9, the spectra was measured by quasi-cw photoinduced absorption. This lock-in technique allows the absorption of long-lived states to be measured with high sensitivity. It is possible to estimate the lifetime of the state using the quasi-cw experiment [46]; however, more accurate methods in-

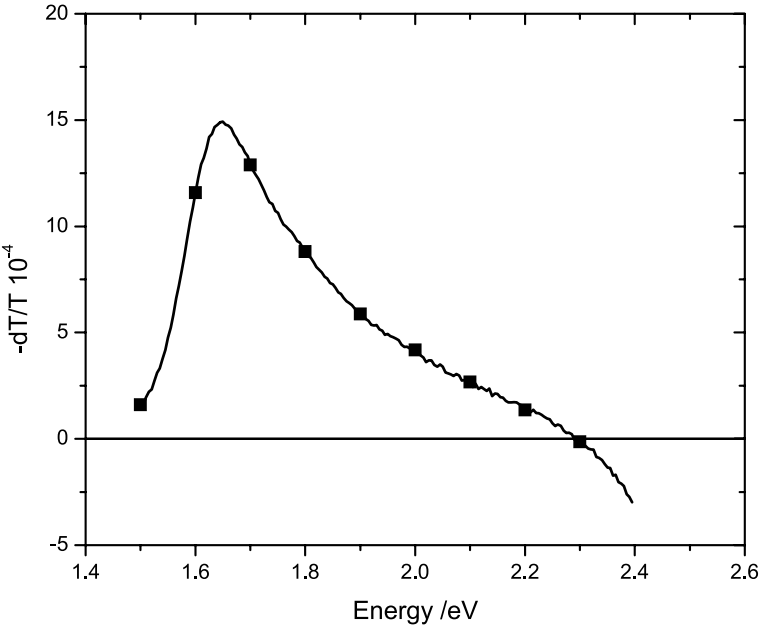

Fig. 9 Excited state absorption spectrum of the triplet exciton of PF2/6

cluding flash photolysis and single wavelength nanosecond photoinduced absorption are preferable given the possibility of multiexponential decays and bimolecular interactions such as triplet–triplet annihilation [24, 28]. Although the peak position at 1.65 eV appears similar to the absorption of the singlet excited state, the feature is confirmed as the absorption of the triplet state by analysis of the lifetime in aerated and degassed solutions. The lifetime is quenched from ~2 ms to 200 ns when oxygen is present in the solution, confirming that the state is of triplet multiplicity [23, 30, 47, 48]. In frozen solution the dynamics of the triplet induced absorption compare favorably with the lifetime of the phosphorescence, also confirming the feature as the triplet induced absorption.

1.5.3 Absorption of the Polyfluorene Charged State (Polaron)

In addition to singlet and triplet excitons there is the possibility that under certain excitation conditions in thin film samples, notably high excitation powers, formation of other long-lived excited states is possible, these are charged species where enough excess energy after photoexcitation causes the electron and hole of the exciton to separate [49] leading to the formation of a pair of polaron-type charge states on adjacent chains, with the opposite sign of charge to conserve overall charge neutrality [50]. Polarons here being elec-

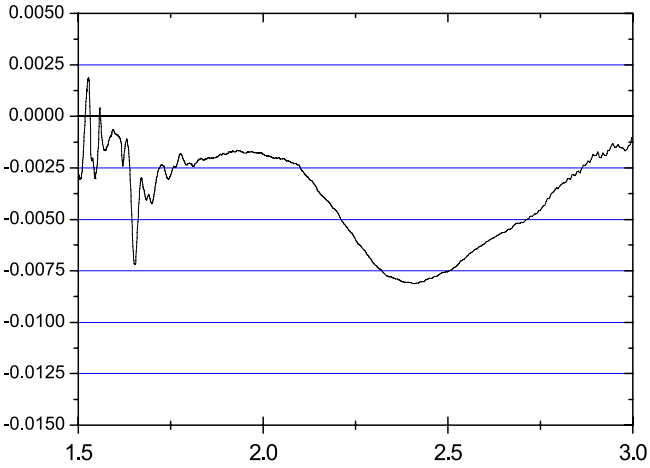

Fig. 10 Transient absorption spectrum of the polyfluorene charged state, in this case free carriers were generated by highly efficient singlet–singlet annihilation; similar spectra are obtained by field induced quenching of polyfluorene singlet states

trons (or holes) coupled to chain deformations [51]. Often these states are "dark" in that they do not directly decay resulting in the emission of light and as such, they are best investigated by absorption techniques. In solution it is also possible to generate charge species, for polyfluorene homopolymers these are a positively charged state of the polymer molecule, i.e. the radical cation, which can be formed by an electron transfer reaction with a strongly electron accepting solvent, such as chloroform. In addition charge states can be formed in thin films of polyfluorene by exciton dissociation in an applied electric field [52] or bimolecular annihilation of singlet excitons [41], the spectrum obtained for the charge states in solid state is also shown in Fig. 10 and this topic is covered in detail in Sect. 3.1.

1.6 Defect Emission

The high fluorescence quantum yield and good thermal stability makes polyfluorenes (PF) one of the more stable blue emitting luminescent polymers. However, it has been observed that light-emitting devices based on polyfluorene tend to degrade showing an undesirable green emission accompanied by an overall decrease of the luminescence intensity [53]. First attributed to interchain interactions such as aggregates and excimers [54], and later explained as resulting from oxidative (keto) defects formed along the polymer backbone and quenching the PF emission [55], the origin of the green emission is still a source of debate within the conjugated polymer community [56, 57]. Figure 11 shows the effect of annealing a PF2/6 film (100 °C

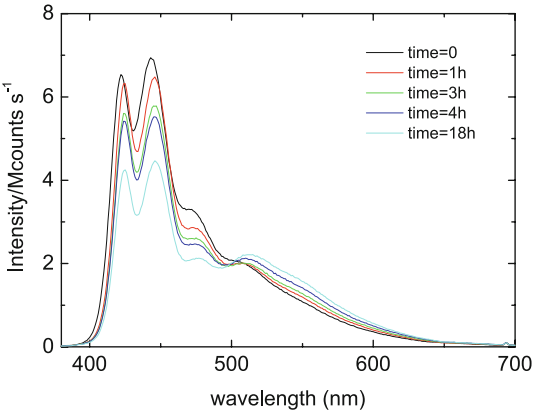

Fig. 11 Fluorescence emission spectra of PFO films obtained at 295 K after being annealed under air

in air), the intensity of the PF emission decreases and a green emission peaking around 530 nm grows over annealing time, showing an isoemissive point around 504 nm.

Synthetic fluorene/fluorenone copolymers [58] show fluorescence emission that matches very well that of degraded films giving strong support to the relation between keto defects and the green emission [57, 59]. Figure 12 shows the emission spectrum of PFO, 9-fluorenone and of a fluorene–fluorenone copolymer with 25% fluorenone groups randomly distributed along the polymer backbone in dilute toluene solution. The green emission does not match that of the simple 9-fluorenone emission, it appears at shorter wavelengths and shows a significantly lower intensity. The PFO emission intensity shows a pronounced decrease when in the presence of fluorenone in the copolymer chain, however this quenching effect does not occur when PFO and 9-fluorenone are simply mixed in solution.

The green emission appears at the expense of PFO emission, indicating that it is quenched by on-chain defects formed between the 9-fluorenone "keto" repeat units and their nearest neighbor fluorene repeat units, forming a delocalized charge transfer state (CTS defect) which decays radiatively to give the green emission [57, 59]. Figure 13, shows the decrease of the PFO emission intensity with increasing the fraction of 9-fluorenone repeat units randomly distributed along the polymer backbone, note the isoemissive point observed around 500 nm, between the PFO and green emissions.

Similar CT states can be formed when PF chains are copolymerized with good charge acceptors. This strategy is now frequently used to improve the charge balance in devices and can have profound impact on the photophysics of these materials via the creation of emissive charge transfer states. Figure 14 shows the absorption and emission spectra, in toluene and chloroform, two solvents with different polarity, of PFO containing dibenzothiophene-

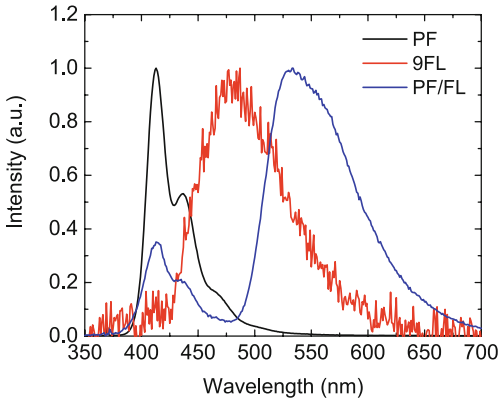

Fig. 12 Normalized fluorescence emission spectra of PFO (*black line*), 9-fluorenone (*red line*) and the fluorene–fluorenone copolymer with 25% 9-fluorenone units ($PF/FL_{0.25}$) (*blue line*)

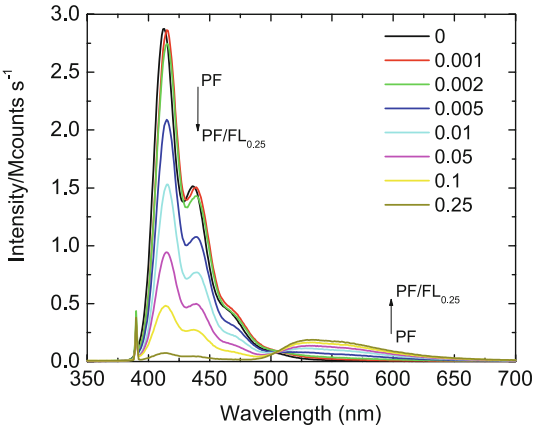

Fig. 13 Fluorescence emission spectra of fluorene–fluorenone copolymers with different 9-fluorenone fractions

S,*S*-dioxide (S) units randomly distributed along the co-polymer backbone (PFS) [60]. The S units are good electron acceptors and charge transfer between the fluorene moieties (F) and the S units occurs during the PFO excited state lifetime. The charge transfer reaction is controlled by the polarity of the surrounding medium and potentially stabilized by conformational changes of the copolymer backbone. As a result the emission profile of PFS copolymers changes from the typical well-resolved blue emission to a broad and red-shifted emission peaking around 460 nm, when going from non-polar to polar medium.

In the solid state, see Fig. 15, the emission of PFS copolymers also appears dependent on the S content. For high S percentages, the emission appears

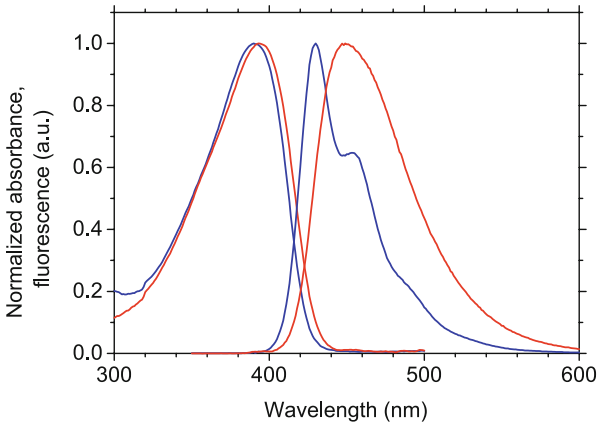

Fig. 14 Normalized absorption and emission spectra of $PFS_{0.3}$ in toluene (*blue line*) and chloroform (*red line*)

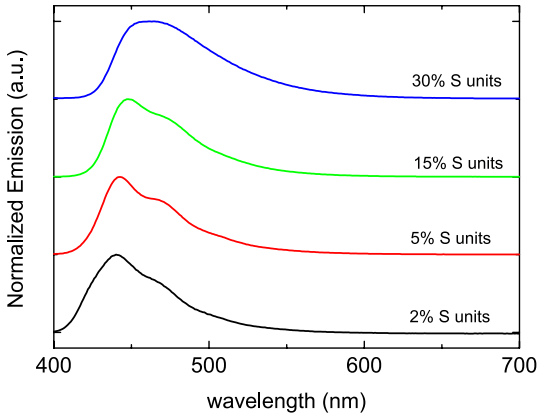

Fig. 15 Normalized fluorescence emission spectra of spin coated thin films on quartz substrates. From *bottom*: $PFS_{0.02}$ (9 mg/mL), $PFS_{0.05}$ (11.2 mg/mL), $PFS_{0.15}$ (9.6 mg/mL), $PFS_{0.3}$ (8.3 mg/mL)

structureless, as it is in a polar medium, but when the S content is low or absent, the emission is structured, as it is in a non-polar environment.

Although the fluorene units are non-polar, the dipole moment in the ground state of the S units is around 5.7 D and the charge transfer reaction increases this value in the excited state. Dipole–dipole interactions between FSF regions in the ground and excited states will thus interact with surrounding S groups of the polymer matrix especially at higher S levels leading to a larger inhomogeneous broadening effect on the emission spectrum of the polymer CT state; at low S levels, the effect is obviously reduced or even non-existent. Thus, the incorporation of co-repeat units that have strong

acceptor or donor character can form stable CT excited states which profoundly alter the photophysics of the co-polymer as compared to the parent homopolymer.

2
Exciton Dynamics

2.1
Singlet Migration

The theoretical framework for exciton migration was established by Bässler and co-workers [61] and in the time-dependent experiments in solid state by Richert et al. [62] and Meskers et al. [2]. Here, energy transfer is associated with an exciton "hopping" motion between localized energetic sites along with initial early time longer range jumps and Forster energy transfer. If initially created with random energy within the inhomogeneously broadened DOS, excitons will preferentially migrate to sites of lower energy, i.e. to the tail states of the DOS. Such down-hill migration is naturally associated with a shift of the average emission energy. For every finite temperature, energetic relaxation terminates once thermally assisted jumps become equally probable to non-assisted jumps to lower energy sites. After this relaxation time no further energetic relaxation is expected. The final emission spectrum is red-shifted and well resolved. The process is also dispersive, as each hop reduces the energy of the exciton, it will take longer for the exciton to be able to make a subsequent jump, thus the hopping decelerates giving a non-linear rate for the process. The main problem with measuring the dynamics of singlet exciton migration is the short period over which the exciton lives before decaying, i.e. several 100 picoseconds to a few nanoseconds. This makes it very difficult to make accurate measurements of the full migration dynamics [63]. To this end, we have found that it is much more informative to study these processes on slower time scales afforded by studying triplet exciton migration which is discussed in the next section. However, by way of illustration to the complexity of the dynamics of singlet excitons, Fig. 16 shows the temperature dependence of Forster transfer between PF2/6 and a tetraphenyl porphyrin dopent [64]. Whereas the dipole–dipole coupling mechanism underlying Forster energy transfer [65] is independent of temperature, excitons at finite temperate may hop and so migrate to within the Forster radius of a trap. At room temperature this gives rise to an anomalously large Forster radius which is seen to decrease at low temperatures. From these measurements an estimate of the hopping rates for singlet excitons in polyfluorene can be derived, at 20 K $0.43 \pm 0.15\ \mathrm{nm}^2/\mathrm{ps}$ and at room temperature, $1.44 \pm 0.25\ \mathrm{nm}^2/\mathrm{ps}$. These values translate into diffusion lengths of 12 nm at 20 K and 22 nm at room temperature. Similar complex migration dynamics are

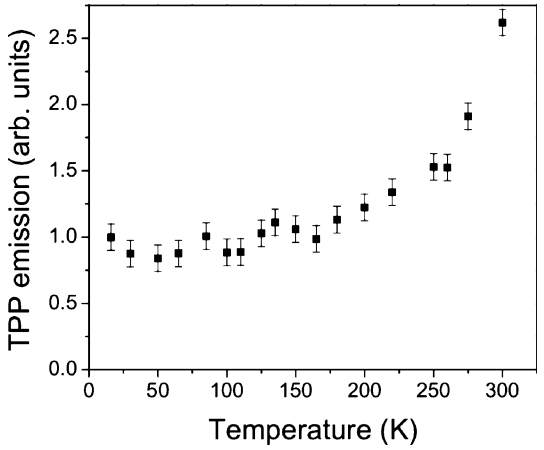

Fig. 16 Temperature dependent emission intensity from TPP dopants in a PF2/6 host. The host is optically excited and the TPP guest is populated by a combination of Forster transfer and exciton migration. Data is corrected for the temperature dependencies of the host and guest photoluminescence quantum yields

also found when studying exciton migration to on-chain keto defects, showing the complex nature of exciton motion in polyfluorenes [66].

2.2 Triplet Diffusion

As we have seen so far, the photophysics of polyfluorenes (and all conjugated polymers) is dominated by their inherent energetic and spatial disorder. This twofold disorder gives rise to time-dependent exciton diffusion i.e. dispersive diffusion so there is no single diffusion constant for the migration of excitons in these polymers. For singlet excitons who have rather short lifetimes, typically a few hundred picoseconds this is hard to show experimentally, but with triplet excitons which have much longer lifetimes this type of migration dynamics can be studied in detail and several earlier theoretical works [62, 67] on non-equilibrium diffusion and energy relaxation in localized state distributions have successfully been applied to triplet diffusion in polyfluorene derivatives [24, 68, 69]. In the framework of these theories the triplet diffusion is treated as a series of incoherent jumps among spatially and energetically localized states. Jumps downhill in energy only depend on the spectral separation of the sites, uphill jumps additionally require thermal activation energy. After pulsed excitation at random energy within the Gaussian DOS the diffusion of the triplet excitons evolve in two fundamentally different migration regimes. Firstly, motion is governed by fast energy relaxation towards low energy sites within the DOS. For the migrating triplet, neighboring sites that allow a next jump (with a lower energy) become fewer after

each successful jump. Consequently, successive jumps to even lower energy sites take longer with the elapse of more and more time after excitation. This renders the diffusion time-dependent or dispersive. The exact behavior of the diffusion, $D(t)$, is strongly dependent on the width of the DOS and the available thermal activation energy, i.e. the temperature of the environment, and is not trivial to cast into an explicit analytical expression. Nevertheless, at zero temperature the following expression has been derived [67]:

$$D(t) \sim \frac{1}{t \ln(\nu_0 t)} \tag{1}$$

which can be approximated by $D(t) \sim t^{-1.04}$ in the long time limit [70]. The time scaling factor ν_0 represents the attempt to jump frequency of the triplet. During this dispersive thermalization period the same zero temperature treatment predicts a temperature independent relaxation of the average energy $\varepsilon(t)$ relative to the center of the Gaussian DOS, which in a simplified version yields [67]:

$$\varepsilon(t) \sim -\sigma \left[\ln\left(\ln \nu_0 t\right)\right]^{1/2} \quad \text{as} \quad t \to \infty\,. \tag{2}$$

Therefore, the relaxation is proportional to the width of the DOS, σ. Furthermore, the time dependent relaxation of the phosphorescence can be measured to actually determine the true width of the triplet DOS of polyfluorene as shown in Fig. 17.

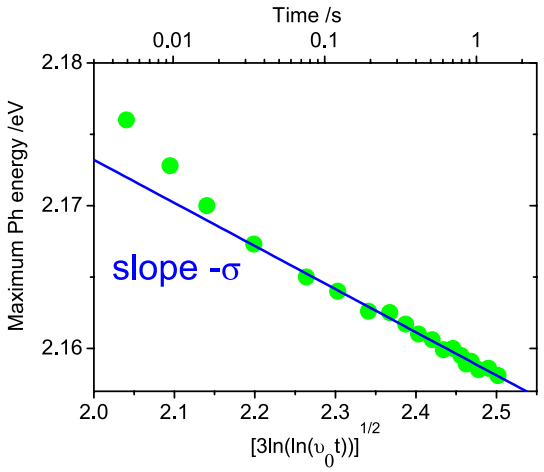

Fig. 17 As the triplet exciton energetically relaxes with increasing time after excitation the Ph spectrum shifts accordingly to lower energies. Here, the peak energies of the phosphorescence spectra of a PF2/6 thin film optically excited at 20 K are plotted according to Eq. 2. The slope yields the true width of the triplet DOS, for polyfluorene ~40 meV. Details are given in [24]

An important implication from Eq. 2 is that the observed phosphorescence spectra are (always) already relaxed within the time resolution of the measurement of phosphorescence spectra. Therefore, the true triplet energy (center of the triplet DOS) is always higher than the apparent phosphorescence spectra, which sets a lower limit only. For PF2/6 the true triplet level is calculated to be 2.26 eV instead of the observed ~2.15 eV [24] from phosphorescence measurement. This higher value however agrees very well with that measured using the pulse radiolysis energy transfer technique which yields triplet energies in the initial unrelaxed state [71].

Even at $T \neq 0$ the excitons, which at $t = 0$ are excited at random within the DOS, initially thermalize to lower energy sites, accordingly in this time period Eqs. 1 and 2 are still valid. However, for finite temperature the diffusivity will approach an equilibrium value after a certain delay time. At this (temperature dependent) segregation time, t_s, the diffusion due to thermalization within the DOS equalizes the thermally activated hopping; afterwards triplet migration is governed by thermally assisted jumps. Now the non-dispersive, classical, regime is attained, which is described by a time-independent, but still temperature dependent, diffusion constant, D_∞. An analytic expression for the segregation time was calculated as [24]:

$$t_s(T) = t_0 \, e^{\left(\frac{c\delta}{k_B T}\right)^2} \tag{3}$$

with $c = 2/3$ for three-dimensional migration [24] and t_0 is related to ν_0 and denotes the dwell time for triplets that migrate through a hypothetical isoenergetic ($\delta = 0$) equivalent structure. Whilst the energetic relaxation as a function of temperature and time of the triplet exciton can be well observed by monitoring phosphorescence spectra, it is more difficult to measure the time or temperature dependent diffusion rate directly. This can only be done indirectly, for example by studying the time dependent emission of emissive triplet acceptors [69]. The triplet diffusion is also the key parameter to understand the dynamics of migration activated triplet–triplet annihilation. For polyfluorene derivatives this issue has been studied in some detail [69] and will be considered in Sect. 3.2.

2.3 Defect Trapping

Time-resolved fluorescence studies of fluorene–fluorenone copolymers in dilute toluene solution, enable us to identify different time regimes in the photoluminescence (PL) decay. Figure 18 shows the results of a maximum entropy method (MEM) analysis of the PL decays of fluorene–fluorenone copolymers [58] collected at the fluorene emission wavelength [66]. The different time regimes of the PL decay are associated with different kinetic species which migrate to the defects, most typically these are the CTS defects

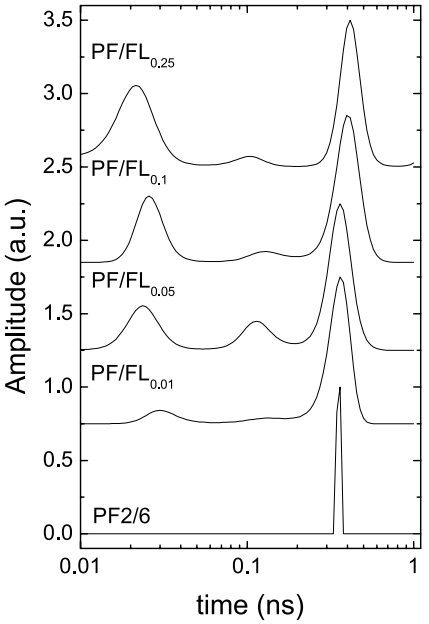

Fig. 18 Maximum entropy method (MEM) analysis of PF2/6 and PF/FLx copolymers. For PF2/6 only a narrow distribution is observed at 360 ps. For PF/FLx copolymers, together with the distribution 60 ps, two additional distributions are observed around 20 and 100 ps

(at keto sites) formed between the fluorenone groups and the nearest neighbor fluorene units, these defects are the acceptors of energy transfer from the polyfluorene donor, alternatively they could be dilute co-monomer units or even intentional dopants. This gives rise to various quenching mechanisms for the fluorene singlet exciton with the quenching occurring in these different time regimes as follows; (1) slow-quenched fluorene singlet excitations (PF_{qslow}), fluorene excitations located far from the traps but free to move along the polymer chains by energy hopping eventually reach a quenching center, (2) unquenched polyfluorene singlet excitations (PF_{unq}), and (3) fast-quenched polyfluorene singlet excitations (PF_{qfast}) where the exciton is created close to a trap and undergoes rapid energy transfer to the trap.

Figure 18, shows the representation of the quenching rate constants associated with both slow (k_1) and fast (k_2) quenching time regimes, also shown is the result from PF2/6 with negligible trap content showing a well-defined single exponential decay time. In the case presented, the slower quenching regime ($k_1 = 1.2 \times 10^{11}\ s^{-1}$) is dependent on the fluorenone fraction, such that with increasing Q it becomes more probable that an excitation finds a CTS defect, analogous to what happens in a diffusive quenching process.

The determination of the quenching rate constant associated with the fast regime k_2, suggests that k_2 can qualitatively be fitted with Eq. 4, with

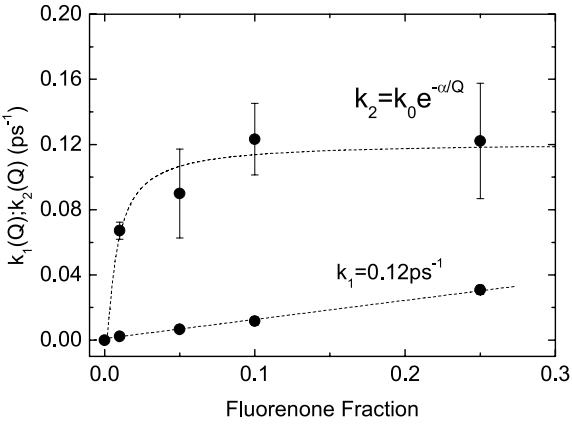

Fig. 19 Determination of k_1 and k_2. The rate constant associated with the slower time regime shows a linear dependence with the fluorenone content. The fast time regime suggests an exponential dependence with fluorenone fraction, compatible with a short range mechanism

$k_0 = 0.12\ \mathrm{ps}^{-1}$ and $\alpha = 0.006$, where k_0 represents the maximum rate constant and α is a parameter without physical meaning, and suggesting the process is described by the Dexter electron exchange mechanism [72]

$$k_2(Q) = k_0\, \mathrm{e}^{-\frac{\alpha}{Q}}\ . \tag{4}$$

Increasing Q, would decrease the average minimum distance between a self localized $PF_{q\text{-fast}}$ excitation and a possible CTS defect, which suggests that Eq. 4, simply describes the qualitative dependence with distance for the Dexter electron exchange mechanism $k_{ET} = k_0\, \mathrm{e}^{-R}$, where k_0 is the maximum rate constant for energy transfer, occurring when donor and acceptor are at the "collision" distance R_0 and R is the separation between donor and acceptor when they are further apart than R_0.

The fact that fitting k_2 with Eq. 4, leads to k_0 equal to k_1, suggests that what is in fact controlling the quenching process is not the energy migration along the chain but instead the energy transfer from PF units to the CTS defects.

2.4 Amplified Spontaneous Emission

In the literature there are extensive reports on the observation of amplified spontaneous emission (ASE) of polyfluorene [73–76]. ASE occurs at high excitation intensities when it is possible to create a transient excited state population which is greater than the population of the lower lying state to which it radiatively decays, i.e. forming a population inversion. If there is some feedback mechanism of emitted photons, stimulated emission can build

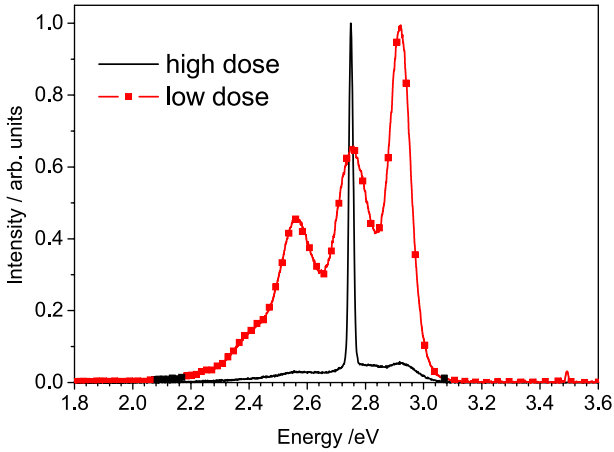

Fig. 20 Normalized emission spectra of a PF2/6 film at 20 K after optical laser excitation with a high and a low pulse intensity of 170 ps duration. The first vibronic overtone, 2.75 eV, of the polyfluorene spectrum undergoes ASE

up and dominate over spontaneous emission. In polymer thin films this is most likely to arise by waveguiding and internal reflection at the substrate interface [76]. However, most of the work has focused on PFO, which is somewhat of a special case and not typical for polyfluorene derivatives, as it has a propensity to form different phases which will be discussed in Sect. 4. As for many other conjugated polymers, typical polyfluorene derivatives, notably PF2/6 and PSBF, ASE exclusively occurs at the energetic position of the first vibronic overtone, i.e. around 2.75 eV at low temperature. A typical example for ASE of PF2/6 is shown in Fig. 20. The 0–0 mode, although of highest intensity, has underlying tail absorption, which quenches the gain, especially over long path lengths through the material typical in a waveguide mode.

3
Exciton–Exciton Interactions

3.1
Singlet–Singlet Annihilation

At high excitation densities in the solid state, the decay of the singlet exciton becomes excitation dependant, bimolecular annihilation of the singlet excitons introduces a fast component to the decay [41, 42, 77, 78], this is shown in Fig. 21. In a number of publications pump-probe spectroscopy has been used to study the phenomena surrounding this accelerated decay. The bimolecular annihilation reaction is effectively energy transfer from one excited singlet to

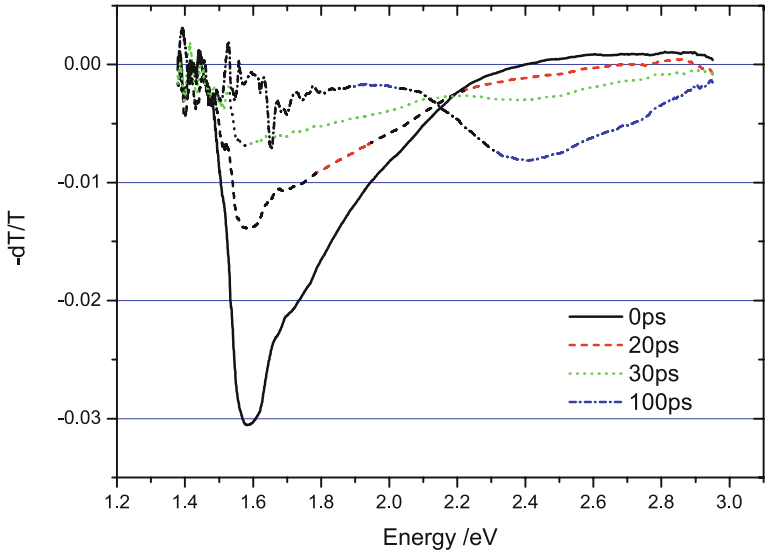

Fig. 21 Pump-probe spectra for the prototypical polyfluorene PF2/6 at high excitation density, showing the photoinduced absorption feature of the singlet population (1.6 eV peak) being rapidly quenched, leading to the formation of charges and characterized by the absorption of the charged state at 2.6 eV

another; thus proceeding in the following way:

$$S_1 + S_1 \longrightarrow S_0 + S_n \,,$$
$$S_n \longrightarrow (1 - \eta)(S_1 + Q) + \eta(p^+ + p^-) \,.$$

The production of a highly excited singlet state has important consequences; while many of the highly excited S_n states decay non-radiatively to the emissive S_1 state, there is also a possibility for the S_n state to dissociate into a pair of charges. The pump-probe spectra in Fig. 21 shows the quenching of the singlet photoinduced absorption spectrum being replaced with the characteristic absorption of the polyfluorene charged state at 2.4 eV. The stable isobestic point shows that there is a direct donor–acceptor relationship between the decay of the upper singlet state and the generation of the charges. This is the principal mechanism for the photogeneration of charge pairs in the solid state. The excitation density dependence of singlet decay is shown at room temperature and at 10 K in Fig. 22, the figure shows the decay of the singlet photoinduced absorption feature at low and high excitation density, the effect of the accelerated decay of the singlet is clear at high excitation density. This effect is quantified in Fig. 23 which shows that although the initial intensity of the excited state absorption remains linear with excitation fluence, the intensity of the absorption after 100 ps follows a linear law

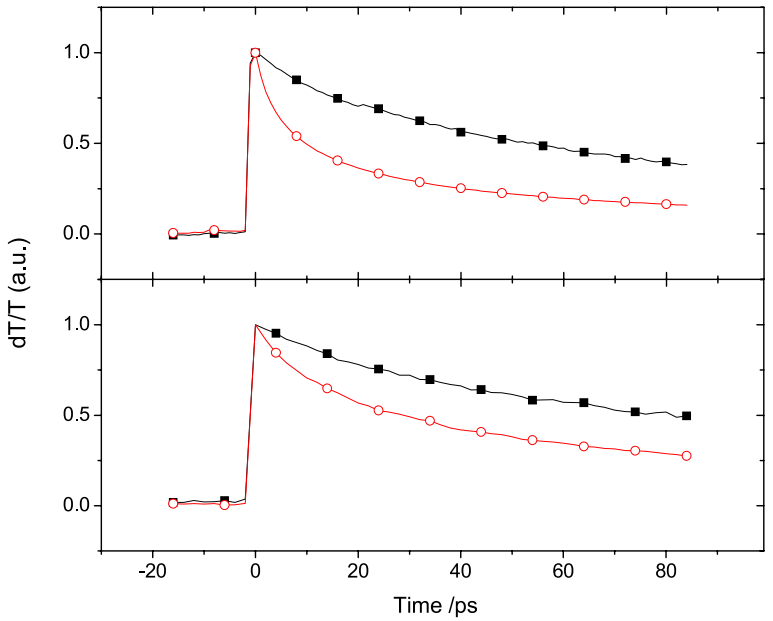

Fig. 22 Decay of the singlet population at 300 K (*top*) and 10 K (*lower*) for high (○) and low (■) excitation density

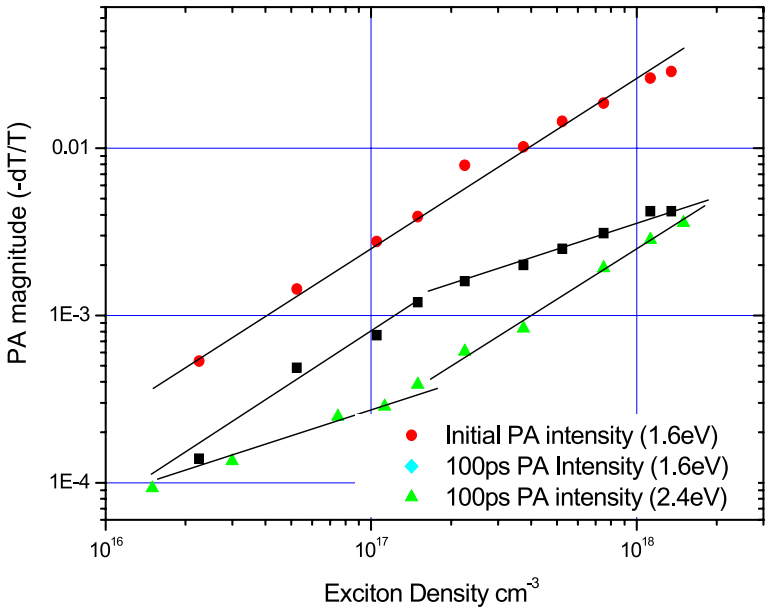

Fig. 23 Excitation density dependence of the photoinduced absorption features in Fig. 21; the threshold for the decay of the singlets being dominated by singlet–singlet annihilation at 1.5×10^{17} cm^{-3} is clear

at low fluence and a quadratic law above a threshold excitation density of 1.5×10^{17} cm^{-3}, where an additional, bimolecular decay process begins to have an effect on the decay of the singlet states. In addition, in the region of the charge state absorption at 2.4 eV there is an increase in the intensity of the absorption at the same point.

The Förster radius for the energy transfer reaction between two excited singlets can be calculated from the overlap of the fluorescence spectrum and the singlet excited state absorption, giving $R_0 = 1.1 \pm 0.5$ nm, which suggests that singlet–singlet annihilation is very inefficient given that the mean separation of the excited states at the observed threshold for the annihilation process is close to 20 nm. This seems to be at variance to the experimental data. The two panels in Fig. 22 showing the excitation dependence of the decay at different temperatures provide the answer; the annihilation becomes possible because at room temperature the singlets are very mobile; exciton diffusion allows the excited states to quickly become close enough to interact and the process remains efficient. At low temperature, the mobility of the singlet excitons drops and the effect of the annihilation becomes less, i.e. singlet–singlet annihilation is also an exciton diffusion controlled process.

3.2 Triplet–Triplet Annihilation and Delayed Fluorescence

With sensitive gated detection an emission contribution, with considerably longer lifetime than the fluorescence lifetime is readily detected in many luminescent polymers, not least polyfluorenes and is termed delayed fluorescence (DF) [79]. It is very frequently observed in studies of polyfluorenes [24, 80] and a typical example is shown in Fig. 24. Using pulse radiolysis, where very high triplet populations can be generated, it is possible to multiply excite single (dilute) chains such that triplet excitons readily migrate and interact on a single chain, annihilate and give strong delayed fluorescence [81]. In general, it may originate from charge carrier recombination (either geminate or non-geminate), inter-system-crossing, or triplet–triplet-annihilation [82]. However, for optical excitation it has been demonstrated that the observed delayed fluorescence of polyfluorene mostly stems from triplet–triplet annihilation [28, 83].

At low temperature, it is reasonable to neglect radiative and non-radiative monomolecular decay and to assume that annihilation is the dominating decay mechanism for the triplets in the time domain much shorter than the triplet lifetime, i.e. for $t < 100$ ms:

$$\mathrm{DF} \sim \frac{\mathrm{d}n_\mathrm{T}}{\mathrm{d}t} = -\gamma_\mathrm{TT} n_\mathrm{T}^2 \tag{5}$$

with n_T being the time-dependent triplet density, γ_TT denotes the triplet–triplet-annihilation "constant". The rate limiting step for the annihilation

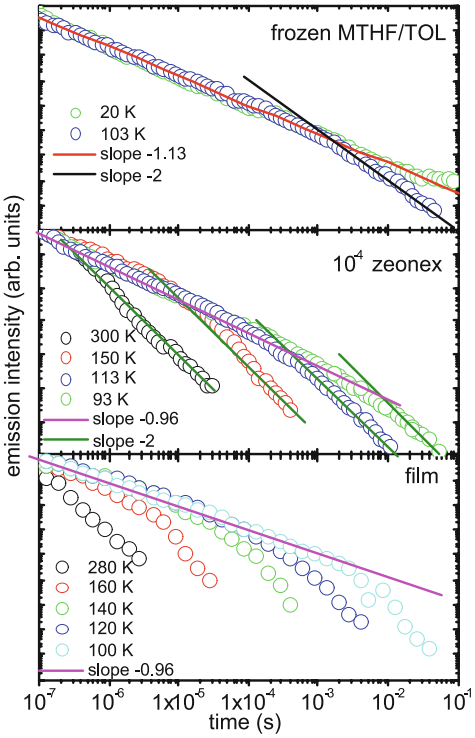

Fig. 24 Delayed fluorescence decays after pulsed optical excitation of PF2/6 as a function of temperature in several media as indicated. Details can be found in [24]

process is triplet exciton migration that brings two triplet excitons within the interaction radius, typically 2 nm. Thus, triplet migration is the key to understanding the dynamics of delayed fluorescence in polyfluorene. If bimolecular triplet annihilation dominates triplet decay then according to Eq. 5 DF and triplet population obey algebraic decay laws with exponents of –2 and –1, respectively. However, according to Eq. 1 at low temperature, during the dispersive time regime the diffusivity of the triplet and thus the triplet annihilation rate slows down with time with a slope of –1. In consequence, the apparent decay of the DF is retarded and features a slope of –1 instead of –2. After the temperature dependent segregation time, Eq. 2, is reached the triplet diffusivity approaches a constant value and so does the triplet annihilation rate. Without the retarding influence from the time dependent triplet annihilation rate, the DF decay proceeds with the classical slope of –2.

Corresponding experimental data for PF2/6 in solid film, frozen solution, and in an inert matrix polymer are shown in Fig. 25. A clear turnover from an initial slope of –1 to a slope of –2 occurs, the turnover occurring earlier for increasing temperature. By analyzing this data according to Eq. 3, such

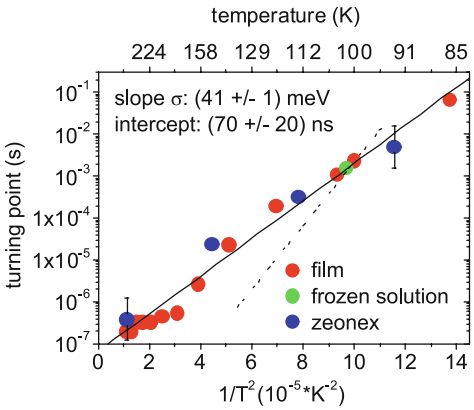

Fig. 25 Presentation of the turn over points between dispersive and non-dispersive triplet diffusion as extracted from Fig. 24 and plotted according to Fig. 3. Details can be found in [24]

as shown in Fig. 25, it is possible to gain the true triplet DOS width and the attempt-to-jump frequency for the triplet exciton, which for PF2/6 works out as 40 meV and 70 ns, respectively [24].

Because of the dispersive nature of the triplet diffusion, the triplet annihilation rate must also be a function of time and temperature. Alternatively, for continuous excitation the annihilation rate becomes a function of excitation dose. Figure 26 shows the saturation of the triplet density during continuous

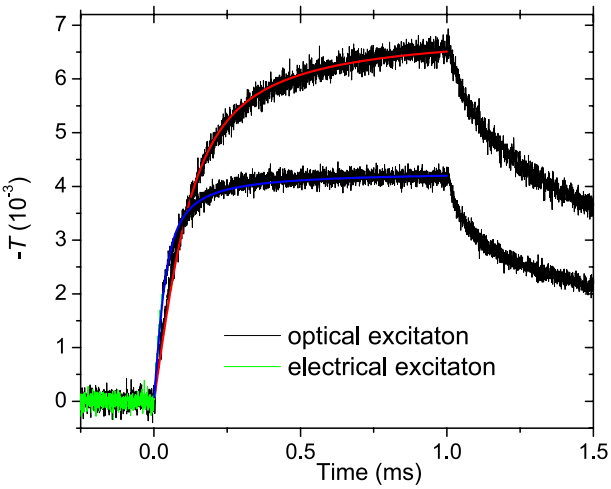

Fig. 26 Transient triplet absorption data of PSBF devices after optical (*black curve*) and electrical (*green curve*) excitation for 1 ms. The *solid lines* are fits according to a model that takes triplet–triplet annihilation into account. Details can be found in [24]

optical and electrical excitation due to triplet–triplet annihilation for a PSBF device. A careful analysis of such data allows an estimation of the triplet annihilation rate at $\gamma_{TT}(I_0) = 1.1 \times 10^{-32} I_0^{0.71} m^3\ s^{-1}$ for PBSF, which is of the order $10^{-15}\ cm^3\ s^{-1}$ for typical excitation doses [68, 84].

3.3 Singlet–Triplet Annihilation

In a similar way to the annihilation of pairs of singlets or pairs of triplets it is theoretically possible for singlet excitons to annihilate with triplets. As with the singlet–singlet annihilation this is theoretically possible as a Förster transfer between the singlet and the triplet. However, although theoretically possible, once again the Förster radius is very small. In the case of S–T annihilation there have been only a few reports of triplets efficiently quenching singlet states in polyfluorene, either in the solid state and in single molecule studies and the efficiency of the observed process is much lower than singlet–singlet annihilation [85, 86]. The efficiency of S–S annihilation is enhanced by the migration of the singlets, but the migration does not seem to dramatically enhance the efficiency of S–T annihilation. One suggestion for this is that the small spatial extent and perpendicular orientation of the triplet compared to the singlet state prevents the states coming close enough for the reaction to take place [35, 41] on an individual chain, and as the Forster radii are rather small, <10 Å, only intra chain events are likely.

4 The "Beta" Phase of Polyfluorene

4.1 Absorption and Emission

A new "phase" of PFO was first observed by Grell and Bradley et al. [87, 88], who reported the appearance of a shoulder at the onset of the absorption band of films of both neat PFO, PFO dispersed in polystyrene and PFO solutions in poor-solvents (such as cyclohexane). This shoulder could, upon appropriate treatment, evolve into a well-defined peak with a maximum at 437 nm as seen in Fig. 27. In particular, it was observed that this peak becomes more prominent in films exposed to solvents or upon their slow warming from 77 K up to room temperature. On the basis of X-ray fiber diffraction studies, Grell et al. [89] concluded that the lower energy state is associated with particularly extended conformations of PFO chains [90], resulting from the polymer response to some physical stress, either driven by solvent quality or temperature [91]. Furthermore, it has been suggested [91] that octyl side-chains in PFO are particularly effective at inducing and stabilizing such

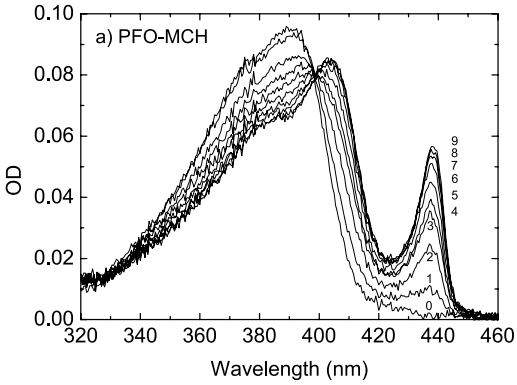

Fig. 27 Growth of a new absorption band below the π–π^* transition in dilute PFO cooled (1 at 295 K to 9 at 130 K) in a poor solvent, MCH. A clear isobestic point is observed indicative of a simple A $\rightarrow$ B reaction and is the signature of the formation of a new morphological state of the PFO in which the polymer chains become rigid and planar. This state has been coined the "beta-phase" [88]

intramolecular ordering in solution, when compared to hexyl and dodecyl side-groups. Recently, the concept of side chain-driven planarization upon polymer agglomeration in solvent mixtures due to an increase of the fraction of a poor-solvent was introduced [92, 93].

Optically, the β-phase is very characteristic. In Fig. 27 a new absorption feature, below the π–π^* transition is seen, typical as a small component but which can be induced to grow especially upon cooling [93]. However, this small band in the absorption spectrum produces profound changes in emission, and in films, emission from the β-phase dominates. β-Phase emission is characterized by a spectrum of very well-defined sharp vibronic replicas with almost no Stokes shift. Indeed the spectrum is very similar to that of a ladder polymer, see Fig. 28. The domination of the β-phase emission comes about through efficient Forster transfer from the "host" PFO to the β-phase inclusions (or guests) in the PFO matrix. Time-resolved energy transfer measurements show this to be a very efficient process [94]. Since the β-phase spectrum is so reminiscent of the ladder polymer emission, it is obvious to conclude that indeed the β-phase is a rigid planar segment of PFO chain, or more likely the β-phase is a fully planar rigid PFO chain.

As with singlet emission, β-phase triplet emission is red shifted compared to that of the PFO to 2.08 eV in thin film at 20 K [23] and the vibronic components are extremely narrow indicting a narrow DOS. In fact, the phosphorescent peaks are ca. 3-times narrower than those measured in a ladder polymer indicating a more homogeneous environment. The ratio of the 0–0 to 0–1 modes in the phosphorescence is very large, with more than 95% of the

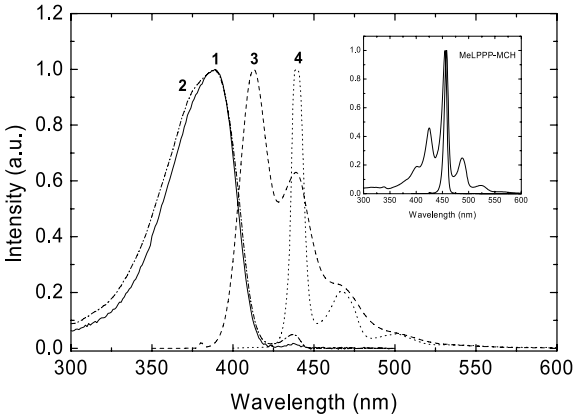

Fig. 28 Emission spectra of cooled and uncooled PFO in MCH. Once the beta phase has formed all emission emanates from this phase. For comparison, the *inset* shows the absorption and emission of rigid MeLPPP

emission being in the 0–0 mode, indicative of a highly planar and rigid backbone conformation. With such a narrow well-defined DOS, both the $T_1 \rightarrow T_n$ and a second transition to a higher lying triplet level can be observed in quasi CW pump probe measurements [23].

4.2 Effect of Alkyl Chain Length

It was originally thought that the β-phase only formed in poly(9,9′-di-*n*-octylfluorene) (PF8) [91, 95], however this is not in fact the case. β-Phase can be induced both in poly(9,9′-di-*n*-septylfluorene) (PF7) and poly(9,9′-di-*n*-nonylfluorene) (PF9) by either cooling solutions (in bad solvent such as MCH) or in cast films [6]. Detailed X-ray and neutron scattering studies on PF7, PF8 and PF9 confirm the presence of 2-D sheet structures associated with the β-phase, in solutions of these polymers [96, 97]. There is also a literature report that a β-phase like state can be induced in poly(9,9′-di-*n*-hexylfluorene) (PF6) [98]. Optical characterization of the β-phase states in PF7 and PF9 confirm that they are very similar to that found in PF8 but they are blue shifted by ca. 7 nm and have different stability over time, with PF8 yielding the most stable β-phase. These findings point to a mechanism of β-phase formation where side chain interactions between adjacent polymer backbones causes interchain "zipping" which has the direct consequence of planarizing the PF backbone, yielding the characteristic β-phase optical properties. This view point is also supported by X-ray results [90].

4.3 Amplified Spontaneous Emission

The β-phase of PFO is probably the most promising conjugated polymer system to achieve true lasing. Here, the emission is concentrated in a very narrow spectral region leading to a large gain at this wavelength. But even more important, the β-phase together with its surrounding non-ordered amorphous polyfluorene matrix constitutes an intrinsic four level system [73]: Singlet exciton excitation in the high energy amorphous PFO host, rapidly leads to excitations being trapped at the low energy β-phase sites [94]. Consequently, the β-phase subsystem is efficiently pumped, and, depending on β-phase concentration within the amorphous phase and excitation dose, excited state

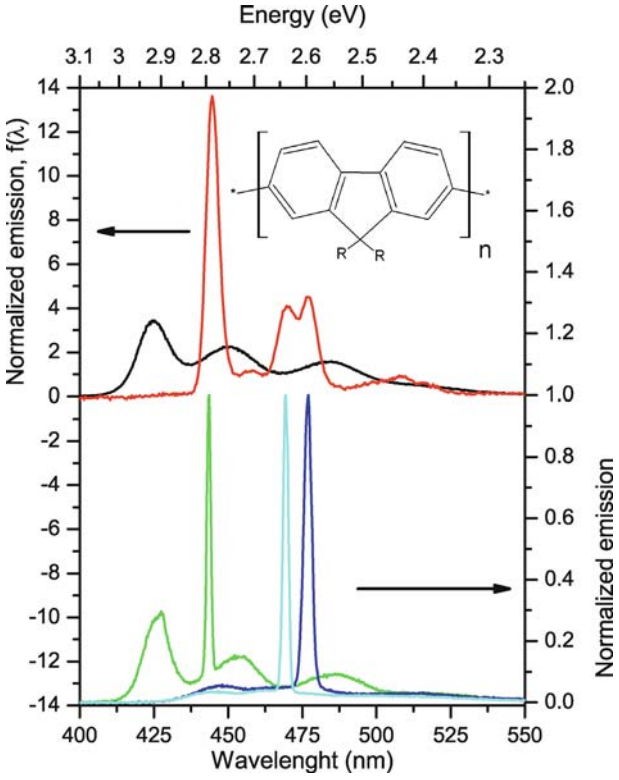

Fig. 29 *Upper panel*: Comparison of amorphous (*black*) and β-phase (*red*) emission spectra taken at 20 K, whereby the integrated emission was normalized. *Lower panel*: Compendium of normalized ASE action spectra of an amorphous film with small amount of β-phase showing ASE to the β-phase ground state (*left narrow peak*) and PFO films with high content of β-phase (*center* and *right narrow peak*) exhibiting lasing to vibronic levels. The chemical repeat unit of PFO is depicted in the inset with R = octyl. Details are given in [73]

inversions have been demonstrated. In this case ASE occurs from the leading 0–0 transition of the β-phase. Given these ideal starting conditions to observe ASE, it is probable that all ASE observed in PFO originates from the β-phase and not intrinsic to amorphous polyfluorene. Figure 29 shows the PL spectra of amorphous and β-phase PFO at low temperature and low excitation dose. For sufficient excitation dose, it is always the β-phase that shows ASE. The ASE wavelength depends on the β-phase concentration within the film, with higher concentrations leading to higher ASE emission wavelength, i.e. from the 0–1 and 0–2 modes [73].

References

1. Kersting R, Lemmer U, Mahrt RF, Leo K, Kurz H, Bassler H, Gobel EO (1993) Femtosecond Energy Relaxation in Pi-Conjugated Polymers. Phys Rev Lett 70(24):3820–3823
2. Meskers SCJ, Hubner J, Oestreich M, Bassler H (2001) Dispersive relaxation dynamics of photoexcitations in a polyfluorene film involving energy transfer: Experiment and Monte Carlo simulations. J Phys Chem B 105(38):9139–9149
3. Grage MML, Wood PW, Ruseckas A, Pullerits T, Mitchell W, Burn PL, Samuel IDW, Sundstrom V (2003) Conformational disorder and energy migration in MEH-PPV with partially broken conjugation. J Chem Phys 118(16):7644–7650
4. Dias FB, Macanita AL, de Melo JS, Burrows HD, Guntner R, Scherf U, Monkman AP (2003) Picosecond conformational relaxation of singlet excited polyfluorene in solution. J Chem Phys 118(15):7119–7126
5. Karabunarliev S, Bittner ER, Baumgarten M (2001) Franck–Condon spectra and electron-libration coupling in para-polyphenyls. J Chem Phys 114(13):5863–5870
6. Bright D, Dias F, Galbrecht F, Scherf U, Monkman A (2008) Alkyl chain length effects of the beta phase in polyfluorene. Adv Func Mat, in press
7. Harrison MG, Moller S, Weiser G, Urbasch G, Mahrt RF, Bassler H, Scherf U (1999) Electro-optical studies of a soluble conjugated polymer with particularly low intrachain disorder. Phys Rev B 60(12):8650–8658
8. Palsson LO, Monkman AP (2002) Measurements of solid-state photoluminescence quantum yields of films using a fluorimeter. Advanced Materials 14(10):757–758
9. Lakowicz JR (1999) Principles of fluorescence spectroscopy. 2nd ed, Kluwer Academic/Plenum, New York, p xxiii, 698
10. Sluch MI, Godt A, Bunz UHF, Berg MA (2001) Excited-state dynamics of oligo(*p*-phenyleneethynylene): Quadratic coupling and torsional motions. J Am Chem Soc 123(26):6447–6448
11. Karabunarliev S, Baumgarten M, Bittner ER, Mullen K (2000) Rigorous Franck–Condon absorption and emission spectra of conjugated oligomers from quantum chemistry. J Chem Phys 113(24):11372–11381
12. Lieser G, Oda M, Miteva T, Meisel A, Nothofer HG, Scherf U, Neher D (2000) Macromolecules 33:4490
13. Scholes GD, Larsen DS, Fleming GR, Rumbles G, Burn PL (2000) Origin of line broadening in the electronic absorption spectra of conjugated polymers: Three-pulse-echo studies of MEH-PPV in toluene. Phys Rev B 61(20):13670–13678

14. Grage MML, Pullerits T, Ruseckas A, Theander M, Inganas O, Sundstrom V (2001) Conformational disorder of a substituted polythiophene in solution revealed by excitation transfer. Chem Phys Lett 339(1–2):96–102
15. Muller JG, Anni M, Scherf U, Lupton JM, Feldmann J (2004) Vibrational fluorescence spectroscopy of single conjugated polymer molecules. Phys Rev B 70(3):035205
16. Bassler H, Schweitzer B (1999) Site-selective fluorescence spectroscopy of conjugated polymers and oligomers. Accounts Chem Res 32(2):173–182
17. Becker W (2005) Advanced Time-Correlated Single Photon Counting Techniques. Springer Series in Chemical Physics Vol. 81
18. Hintschich SI, Dias FB, Monkman AP (2006) Dynamics of conformational relaxation in photoexcited oligofluorenes and polyfluorene. Phys Rev B 74(4)
19. Di Paolo RE, de Melo JS, Pina J, Burrows HD, Morgado J, Macanita AL (2007) Conformational relaxation of *p*-phenylenevinylene trimers in solution studied by picosecond time-resolved fluorescence. Chem Phys Chem 8(18):2657–2664
20. Dhoot AS, Ginger DS, Beljonne D, Shuai Z, Greenham NC (2002) Triplet formation and decay in conjugated polymer devices. Chem Phys Lett 360(3–4):195–201
21. Wohlgenannt M, Tandon K, Mazumdar S, Ramasesha S, Vardeny ZV (2001) Formation cross-sections of singlet and triplet excitons in pi-conjugated polymers. Nature 409(6819):494–497
22. Rothe C, King S, Al Attar HA, Monkman AP (2006) Direct measurement of the singlet generation yield in polymer light emitting diodes. Phys Rev Lett 97:076602
23. Rothe C, King SM, Dias F, Monkman AP (2004) Triplet exciton state and related phenomena in the beta-phase of poly(9,9-dioctyl)fluorene. Phys Rev B 70(19):195213
24. Rothe C, Monkman AP (2003) Triplet exciton migration in a conjugated polyfluorene. Phys Rev B 68(7):075208
25. Sinha S, Rothe C, Guntner R, Scherf U, Monkman AP (2003) Electrophosphorescence and delayed electroluminescence from pristine polyfluorene thin-film devices at low temperature. Phys Rev Lett 90(12):127402
26. Monkman AP, Burrows HD, Hartwell LJ, Horsburgh LE, Hamblett I, Navaratnam S (2001) Triplet energies of pi-conjugated polymers. Phys Rev Lett 86(7):1358–1361
27. Monkman AP, Burrows HD, Miguel MD, Hamblett I, Navaratnam S (2001) Triplet state spectroscopy of conjugated polymers studied by pulse radiolysis. Synthetic Metals 116(1–3):75–79
28. Hertel D, Bassler H, Guentner R, Scherf U (2001) Triplet–triplet annihilation in a poly(fluorene)-derivative. J Chem Phys 115(21):10007–10013
29. Rothe C, Brunner K, Bach I, Heun S, Monkman AP (2005) Effects of triplet exciton confinement induced by reduced conjugation length in polyspirobifluorene copolymers. J Chem Phys 122(8):084706
30. King S, Rothe C, Monkman A (2004) Triplet build in and decay of isolated polyspirobifluorene chains in dilute solution. J Chem Phys 121(21):10803–10808
31. Burrows HD, de Melo JS, Serpa C, Arnaut LG, Monkman AP, Hamblett I, Navaratnam S (2001) S-1 similar to >T-1 intersystem crossing in pi-conjugated organic polymers. J Chem Phys 115(20):9601–9606
32. King SM, Rothe C, Dai D, Monkman AP (2006) Femtosecond ground state recovery: Measuring the intersystem crossing yield of polyspirobifluorene. J Chem Phys 124(23):234903
33. Rothe C, King S, Monkman A (2006) Long-range resonantly enhanced triplet formation in luminescent polymers doped with iridium complexes. Nat Mater 5(6):463–466

34. Rothe C, Guentner R, Scherf U, Monkman AP (2001) Trap influenced properties of the delayed luminescence in thin solid films of the conjugated polymer poly(9,9-di(ethylhexyl)fluorene). J Chem Phys 115(20):9557–9562
35. King SM, Vaughan HL, Monkman AP (2007) Orientation of triplet and singlet transition dipole moments in polyfluorene, studied by polarised spectroscopies. Chem Phys Lett 440(4–6):268–272
36. Shank CV, Ippen EP, Fork RL, Migus A, Kobayashi T (1980) Application of Subpicosecond Optical Techniques to Molecular-Dynamics. Philosophical Transactions of the Royal Society of London Series a – Mathematical Physical and Engineering Sciences 298(1439):303–308
37. Tong M, Sheng CX, Vardeny ZV (2007) Nonlinear optical spectroscopy of excited states in polyfluorene. Phys Rev B 75(12)
38. Kraabel B, Klimov VI, Kohlman R, Xu S, Wang HL, McBranch DW (2000) Unified picture of the photoexcitations in phenylene-based conjugated polymers: Universal spectral and dynamical features in subpicosecond transient absorption. Phys Rev B 61(12):8501–8515
39. Virgili T, Cerullo G, Luer L, Lanzani G, Gadermaier C, Bradley DDC (2003) Understanding fundamental processes in poly(9,9-dioctylfluorene) light-emitting diodes via ultrafast electric-field-assisted pump-probe spectroscopy. Phys Rev Lett 90(24):247402
40. Virgili T, Marinotto D, Manzoni C, Cerullo G, Lanzani G (2005) Ultrafast intrachain photoexcitation of polymeric semiconductors. Phys Rev Lett 94(11)
41. King SM, Dai D, Rothe C, Monkman AP (2007) Exciton annihilation in a polyfluorene: Low threshold for singlet–singlet annihilation and the absence of singlet–triplet annihilation. Phys Rev B 76(8)
42. Maniloff ES, Klimov VI, McBranch DW (1997) Intensity-dependent relaxation dynamics and the nature of the excited-state species in solid-state conducting polymers. Phys Rev B 56(4):1876–1881
43. Stevens MA, Silva C, Russell DM, Friend RH (2001) Exciton dissociation mechanisms in the polymeric semiconductors poly(9,9-dioctylfluorene) and poly(9,9-dioctylfluorene-*co*-benzothiadiazole). Phys Rev B 6316(16):165213
44. King SM, Hintschich SI, Dai D, Rothe C, Monkman AP (2007) Spiroconjugation-enhanced intramolecular charge-transfer state formation in a polyspirobifluorene homopolymer. J Phys Chem C 111:18759–18764
45. Beljonne D, Pourtois G, Silva C, Hennebicq E, Herz LM, Friend RH, Scholes GD, Setayesh S, Mullen K, Bredas JL (2002) Interchain vs. intrachain energy transfer in acceptor-capped conjugated polymers. Proc Natl Acad Sci USA 99(17):10982–10987
46. Oconnor P, Tauc J (1982) Photoinducedmidgap Absorption in Tetrahedrally Bonded Amorphous-Semiconductors. Phys Rev B 25(4):2748–2766
47. Cadby AJ, Lane PA, Mellor H, Martin SJ, Grell M, Giebeler C, Bradley DDC, Wohlgenannt M, An C, Vardeny ZV (2000) Film morphology and photophysics of polyfluorene. Phys Rev B 62(23):15604–15609
48. Ford TA, Avilov I, Beljonne D, Greenham NC (2005) Enhanced triplet exciton generation in polyfluorene blends. Phys Rev B 71(12)
49. Kersting R, Lemmer U, Deussen M, Bakker HJ, Mahrt RF, Kurz H, Arkhipov VI, Bassler H, Gobel EO (1994) Ultrafast Field-Induced Dissociation of Excitons in Conjugated Polymers. Phys Rev Lett 73(10):1440–1443
50. Conwell EM, Mizes HA (1995) Photogeneration of Polaron Pairs in Conducting Polymers. Phys Rev B 51(11):6953–6958
51. Bredas JL, Street GB (1985) Polarons, Bipolarons, and Solitons in Conducting Polymers. Accounts of Chemical Research 18(10):309–315

52. Cabanillas-Gonzalez J, Antognazza MR, Virgili T, Lanzani G, Gadermaier C, Sontag M, Strohriegl P (2005) Two-step field-induced singlet dissociation in a fluorene trimer. Phys Rev B 71(15)
53. Montilla F, Mallavia R (2007) On the origin of green emission bands in fluorene-based conjugated polymers. Adv Funct Mater 17(1):71–78
54. Bliznyuk VN, Carter SA, Scott JC, Klarner G, Miller RD, Miller DC (1999) Electrical and photoinduced degradation of polyfluorene based films and light-emitting devices. Macromolecules 32(2):361–369
55. Gaal M, List EJW, Scherf U (2003) Excimers or emissive on-chain defects? Macromolecules 36(11):4236–4237
56. Hintschich SI, Rothe C, Sinha S, Monkman AP, de Freitas PS, Scherf U (2003) Population and decay of keto states in conjugated polymers. J Chem Phys 119(22):12017–12022
57. Dias FB, Maiti M, Hintschich SI, Monkman AP (2005) Intramolecular fluorescence quenching in luminescent copolymers containing fluorenone and fluorene units: A direct measurement of intrachain exciton hopping rate. J Chem Phys 122(5):054904
58. de Freitas PS, Scherf U, Collon M, List EJW (2002) (9,9-Dialkylfluorene-*co*-fluorenone) copolymers containing low fluorenone fractions as model systems for degradation-induced changes in polyfluorene-type semiconducting materials. E-Polymers, ARTN 009, 2002
59. Zojer E, Pogantsch A, Hennebicq E, Beljonne D, Bredas JL, de Freitas PS, Scherf U, List EJW (2002) Green emission from poly(fluorene)s: The role of oxidation. J Chem Phys 117(14):6794–6802
60. Dias FB, Pollock S, Hedley G, Palsson LO, Monkman A, Perepichka II, Perepichka IF, Tavasli M, Bryce MR (2006) Intramolecular charge transfer assisted by conformational changes in the excited state of fluorene-dibenzothiophene-*S*,*S*-dioxide *co*-oligomers. J Phys Chem B 110(39):19329–19339
61. Meskers SCJ, Hubner J, Oestreich M, Bassler H (2001) Time-resolved fluorescence studies and Monte Carlo simulations of relaxation dynamics of photoexcitations in a polyfluorene film. Chem Phys Lett 339(3–4):223–228
62. Richert R, Bassler H, Ries B, Movaghar B, Grunewald M (1989) Frustrated Energy Relaxation in an Organic Glass. Phil Magazine Lett 59(2):95–102
63. Mollay B, Lemmer U, Kersting R, Mahrt RF, Kurz H, Kauffman HF, Bassler H (1994) Dynamics of Singlet Excitations in Conjugated Polymers – Poly(Phenylenevinylene) and Poly(Phenylphenylenevinylene). Phys Rev B 50(15):10769–10779
64. Lyons BP, Monkman AP (2005) The role of exciton diffusion in energy transfer between polyfluorene and tetraphenyl porphyrin. Phys Rev B 71(23):235201
65. Forster T (1948) Zwischenmolekulare Energiewanderung und Fluoreszenz. Annalen Der Physik 2(1–2):55–75
66. Dias FB, Knaapila M, Monkman AP, Burrows HD (2006) Fast and slow time regimes of fluorescence quenching in conjugated polyfluorene–fluorenone random copolymers: The role of exciton hopping and dexter transfer along the polymer backbone. Macromolecules 39(4):1598–1606
67. Grunewald M, Pohlmann B, Movaghar B, Wurtz D (1984) Theory of Non-Equilibrium Diffusive Transport in Disordered Materials. Philosophical Magazine B – Physics of Condensed Matter Statistical Mechanics Electronic Optical and Magnetic Properties 49(4):341–356
68. Rothe C, Al Attar HA, Monkman AP (2005) Absolute measurements of the triplet–triplet annihilation rate and the charge-carrier recombination layer thickness in

working polymer light-emitting diodes based on polyspirobifluorene. Phys Rev B 72(15):155330
69. Rothe C, King S, Monkman AP (2006) Systematic study of the dynamics of triplet exciton transfer between conjugated host polymers and phosphorescent iridium (III) guest emitters. Phys Rev B 73:245208
70. Karg S, Riess W, Dyakonov V, Schwoerer M (1993) Electrical and Optical Characterization of Poly(Phenylene-Vinylene) Light-Emitting-Diodes. Synthetic Metals 54(1–3):427–433
71. Burrows HD, de Melo JS, Serpa C, Arnaut LG, Miguel MD, Monkman AP, Hamblett I, Navaratnam S (2002) Triplet state dynamics on isolated conjugated polymer chains. Chem Phys 285(1):3–11
72. Dexter DL (1953) A Theory of Sensitized Luminescence in Solids. J Chem Phys 21(5):836–850
73. Rothe C, Galbrecht F, Scherf U, Monkman A (2006) The beta-phase of poly(9,9-dioctylfluorene) as a potential system for electrically pumped organic lasing. Advanced Materials 18(16):2137–2141
74. Takahashi H, Naito H (2005) Amplified spontaneous emission from fluorene-based copolymer wave guides. Thin Solid Films 477(1–2):53–56
75. Long X, Grell M, Malinowski A, Bradley DDC, Inbasekaran M, Woo EP (1998) Spectral narrowing phenomena in the emission from a conjugated polymer. Opt Mater 9 (1–4):70–76
76. Scherf U, Riechel S, Lemmer U, Mahrt RF (2001) Conjugated polymers: lasing and stimulated emission. Curr Opin Solid State Mater Sci 5(2–3):143–154
77. Daniel C, Herz LM, Silva C, Hoeben FJM, Jonkheijm P, Schenning A, Meijer EW (2003) Exciton bimolecular annihilation dynamics in supramolecular nanostructures of conjugated oligomers. Phys Rev B 68(23)
78. Martini IB, Smith AD, Schwartz BJ (2004) Exciton–exciton annihilation and the production of interchain species in conjugated polymer films: Comparing the ultrafast stimulated emission and photoluminescence dynamics of MEH-PPV. Phys Rev B 69(3)
79. Sternlicht H, Robinson GW, Nieman GC (1963) Triplet–Triplet Annihilation and Delayed Fluorescence in Molecular Aggregates. J Chem Phys 38(6):1326–1335
80. Rothe C, Palsson LO, Monkman AP (2002) Singlet and triplet energy transfer in a benzil-doped, light emitting, solid-state conjugated polymer. Chem Phys 285(1):95–101
81. Monkman AP, Burrows HD, Hamblett I, Navaratnam S (2001) Intra-chain triplet–triplet annihilation and delayed fluorescence in soluble conjugated polymers. Chem Phys Lett 340(5–6):467–472
82. Pope M, Swenberg CE (1999) Electronic Processes in Organic Crystals and Polymers. Oxford University Press, Oxford, pp 161–166
83. Rothe C, Monkman A (2002) Dynamics and trap-depth distribution of triplet excited states in thin films of the light-emitting polymer poly(9,9-di(ethylhexyl)fluorene). Phys Rev B 65(7):073201
84. Rothe C, King SM, Monkman AP (2006) Direct measurement of the singlet generation yield in polymer light-emitting diodes. Phys Rev Lett 97(7):076602-1–076602-4
85. Zaushitsyn Y, Jespersen KG, Valkunas L, Sundstrom V, Yartsev A (2007) Ultrafast dynamics of singlet–singlet and singlet–triplet exciton annihilation in poly(3-2′-methoxy-5′-octylphenyl)thiophene films. Phys Rev B 75(19):195201-1–195201-7
86. List EJW, Scherf U, Mullen K, Graupner W, Kim CH, Shinar J (2002) Direct evidence for singlet–triplet exciton annihilation in pi-conjugated polymers. Phys Rev B 66(23):235203-1–235203-5

87. Bradley DDC, Grell M, Long X, Mellor H, Grice A, Inbasekaran M, Woo EP (1997) Influence of aggregation on the optical properties of a polyfluorene. Opt Probes Conjugated Polym 3145:254–259
88. Grell M, Bradley DDC, Long X, Chamberlain T, Inbasekaran M, Woo EP, Soliman M (1998) Chain geometry, solution aggregation and enhanced dichroism in the liquid-crystalline conjugated polymer poly(9,9-dioctylfluorene). Acta Polymerica 49(8):439–444
89. Grell M, Bradley DDC, Ungar G, Hill J, Whitehead KS (1999) Interplay of physical structure and photophysics for a liquid crystalline polyfluorene. Macromolecules 32(18):5810–5817
90. Brinkmann M (2007) Directional epitaxial crystallization and tentative crystal structure of poly (9,9′-di-*n*-octyl-2,7-fluorene). Macromolecules 40:7532–7541
91. Teetsov J, Fox MA (1999) Photophysical characterization of dilute solutions and ordered thin films of alkyl-substituted polyfluorenes. J Mater Chem 9(9):2117–2122
92. Scherf U, List EJW (2002) Semiconducting polyfluorenes – Towards reliable structure-property relationships. Advanced Materials 14(7):477–487
93. Dias FB, Morgado J, Macanita AL, da Costa FP, Burrows HD, Monkman AP (2006) Kinetics and thermodynamics of poly(9,9-dioctylfluorene) beta-phase formation in dilute solution. Macromolecules 39(17):5854–5864
94. Ariu M, Sims M, Rahn MD, Hill J, Fox AM, Lidzey DG, Oda M, Cabanillas-Gonzalez J, Bradley DDC (2003) Exciton migration in beta-phase poly(9,9-dioctylfluorene). Phys Rev B 67(19):195333
95. Chunwaschirasiri W, Tanto B, Huber DL, Winokur MJ (2005) Chain conformations and photoluminescence of poly(di-*n*-octylfluorene). Physical Rev Lett 94(10):107402-1–107402-4
96. Knaapila M, Dias FB, Garamus VM, Almasy L, Torkkeli M, Leppanen K, Galbrecht F, Preis E, Burrows HD, Scherf U, Monkman AP (2007) Influence of side chain length on the self-assembly of hairy-rod poly(9,9-dialkylfluorene)s in the poor solvent methylcyclohexane. Macromolecules 40:9398–9405
97. Knaapila M, Garamus VM, Dias FB, Almasy L, Galbrecht F, Charas A, Morgado J, Burrows HD, Scherf U, Monkman AP (2006) Influence of solvent quality on the self-organization of archetypical hairy rods – Branched and linear side chain polyfluorenes: Rodlike chains versus beta-sheets in solution. Macromolecules 39(19):6505–6512
98. Chen SH, Su AC, Su CH, Chen SA (2006) Phase behavior of poly(9,9-di-*n*-hexyl-2,7-fluorene). J Phys Chem B 110(9):4007–4013